Structure of the catalytic, inorganic core of oxygen-evolving photosystem II at 1.9 Å resolution

Keisuke Kawakami[1,], Yasufumi Umena[1,†], Nobuo Kamiya[1,*], Jian-Ren Shen[2,*]

[1]Department of Chemistry, Graduate School of Science, and The OCU Advanced Research Institute for Natural Science and Technology (OCARINA), Osaka City University, Sumiyoshi, Osaka 558-8585, Japan; [2]Division of Bioscience, Graduate School of Natural Science and Technology/Faculty of Science, Okayama University, Okayama 700-8530, Japan.

[†]Present address: Institute for Protein Research, Osaka University, Suita, Osaka, Japan.

[*]Corresponding authors: shen@cc.okayama-u.ac.jp; nkamiya@sci.osaka-cu.ac.jp

Keywords: crystal structure; membrane protein structure; oxygen-evolving complex; photosystem II; water-oxidation

Abbreviations: EXAFS, extended X-ray absorption fine structure; OEC, oxygen-evolving complex; PSII, photosystem II; RC, reaction center.

Abstract

The catalytic center for photosynthetic water-splitting consists of 4 Mn atoms and 1 Ca atom and is located near the lumenal surface of photosystem II. So far the structure of the Mn_4Ca-cluster has been studied by a variety of techniques including X-ray spectroscopy and diffraction, and various structural models have been proposed. However, its exact structure is still unknown due to the limited resolution of crystal structures of PSII achieved so far, as well as possible radiation damages that might have occurred. Very recently, we have succeeded in solving the structure of photosystem II at 1.9 Å, which yielded a detailed picture of the Mn_4CaO_5-cluster for the first time. In the high resolution structure, the Mn_4CaO_5-cluster is arranged in a distorted chair form, with a cubane-like structure formed by 3 Mn and 1 Ca, 4 oxygen atoms as the distorted base of the chair, and 1 Mn and 1 oxygen atom outside of the cubane as the back of the chair. In addition, 4 water molecules were associated with the cluster, among which, 2 are associated with the terminal Mn atom and 2 are associated with the Ca atom. Some of these water molecules may therefore serve as the substrates for water-splitting. The high resolution structure of the catalytic center provided a solid basis for elucidation of the mechanism of photosynthetic water splitting. We review here the structural features of the Mn_4CaO_5-cluster analyzed at 1.9 Å resolution, and compare them with the structures reported previously.

Introduction

Photosystem II (PSII) catalyzes photo-induced water oxidation leading to the production of protons and molecular oxygen, the latter of which is indispensable for sustaining oxygenic life on the earth. Cyanobacterial PSII is composed of 17 membrane-spanning subunits and 3 peripheral, membrane-extrinsic subunits with a total molecular weight of 350 kDa [1,2]. The catalytic center for water oxidation is a Mn_4Ca-cluster containing 4 Mn atoms and 1 Ca atom located in the lumenal surface of the thylakoid membrane, which cycles through the S_i-states (i=0-4) [3,4] upon abstraction of electrons by the PSII reaction center (RC) (for a review, see 5). In the last decade, the structure of PSII has been solved by 3 groups independently at resolutions ranging from 2.9 -3.8 Å, from two closely related thermophilic cyanobacteria *Thermosynechococcus elongatus* [6-9] and *T. vulcanus* [10-12]. These structural studies identified the location of all of the protein subunits, as well as the location and arrangement of most of the cofactors, and provided the basis for further elucidation of the mechanisms of energy absorption and migration, electron transfer, and water oxidation reactions taking place within PSII. The resolutions achieved so far, however, were not high enough to allow a detailed determination of the precise structure of the Mn_4Ca-cluster that constitutes the catalytic center of the oxygen-evolving complex (OEC), as well as some of the amino acid side chains and cofactors. In addition, the Mn_4Ca-cluster suffered from X-ray radiation damage during collection of the X-ray diffraction data [13,14]. Thus, there were some differences in the geometric arrangement as well as their ligation pattern of the Mn_4Ca-cluster in the structures reported so far [6-11,15-20], and virtually no bridging oxygen between the metal atoms has been observed experimentally by X-ray crystallography. Furthermore, no water molecules, which are important as substrates and ligands of the Mn_4Ca-cluster, have been located clearly in the structures reported so far.

In order to uncover the mechanism of light-induced water oxidation, it is essential to solve the detailed structure of the Mn_4Ca-cluster, as well as to locate the water molecules that may serve as the substrate for the reaction. In order to achieve this goal, we screened the crystallization conditions for PSII dimers purified from *T. vulcanus* extensively, and optimized the conditions for post-crystallization treatments and crystal harvesting. As a result, we succeeded in improving the crystal resolution to 1.9 Å [21], a

resolution significantly higher than those reported previously. In order to reduce the possible X-ray radiation damage, we employed a sliding-oscillation method to reduce the X-ray dose illuminated on a unit volume of a crystal. This gave rise to a low dose data set which was processed to a resolution of 1.9 Å. The electron density map calculated based on this data set showed well defined shapes for each of the metal atoms in the Mn_4Ca-cluster, which were well separated from each other, allowing an unambiguous determination of the locations of all of the metal atoms [21]. The crystallographic *B* factors for each of the metal atoms ranged from 22.8-28.6 $Å^2$, and were lower than the average *B* factor of 35.2 $Å^2$ for the whole PSII dimer structure at 1.9 Å resolution [21]. This suggests that no significant radiation damage had occurred with the Mn_4Ca cluster during our experiment. In the following, we describe the detailed structure of the Mn_4Ca-cluster, and compare it with the previous structures.

Locations of the metal ions in the Mn_4Ca-cluster

In the electron density map reported so far, the 5 metal ions of the Mn_4Ca-cluster were not separated, leading to a ball-like shape of the electron density for the whole 5 metal ions [6-11]. This makes the precise identification of positions of the individual atoms impossible based solely on the X-ray diffraction results. Thus, the structural model of the metal cluster was built partially based on the distance information derived from EXAFS studies [15, 22-25] with the optimization from theoretical calculations [16-20]. However, it is difficult to assign a specific distance to a certain pair of the metal ions. In the 1.9 Å resolution map obtained (Fig. 1A), the electron densities for the individual metal ions were clearly separated, allowing an unambiguous identification of each of the metal atoms [21]. Furthermore, the electron density for the Ca atom was lower than the 4 Mn atoms, allowing us to distinguish between the Ca and Mn atoms. The lower electron density is most likely due to the lower number of electrons of the Ca atom than that of the Mn atoms (The atomic number of Ca is 20 and that of Mn is 25. Assuming Ca is in a Ca^{2+} state and Mn in Mn^{3+} or Mn^{4+} states, the number of electrons of the Ca ion is 18, and the number of electrons of the Mn ions is 21-22.).

Based on the locations of the 5 metal ions determined at 1.9 Å resolution, the distances between each pair of Mn-Mn and Mn-Ca atoms could be determined, which is shown in Fig. 1B [21]. There were 3 short distances between 3 Mn-Mn pairs, which are

2.8 Å of Mn1-Mn2, 2.9 Å of Mn2-Mn3, and 3.0 Å of Mn3-Mn4. These are slightly longer than the 3 short distances reported from EXAFS studies. However, if we consider that there is an error of 0.16 Å in the distances of the X-ray structure [21], we can consider that the 3 short distances determined at 1.9 Å resolution are very similar to those reported from the EXAFS studies [15,22-25]. The shortest distances between Ca-Mn are two 3.4 Å and one 3.5 Å; these are also similar to the short distance of 3.3-3.4 Å for Ca-Mn reported from the EXAFS studies, although in the EXAFS studies the exact number of the short distances between the Ca-Mn atoms were difficult to be determined [26-27].

The positions of the 5 metal ions determined at 1.9 Å resolution were compared with those reported at 3.5 Å resolution by Barber and his co-workers [7] and at 2.9 Å resolution by Zouni and co-workers [9]. As can be seen in Fig. 1C, the positions of the 4 Mn atoms determined by Zouni et al. at 2.9 Å resolution are rather similar to those determined at the 1.9 Å resolution. A slightly large difference was found in the position of the Ca atom between the two structures, leading to a rather large difference in the distance between Ca and Mn atoms (Table 1). On the other hand, rather large differences were found in the positions of all of the 5 metal atoms between the structures determined at 3.5 Å and 1.9 Å resolutions, leading to large differences in the distances among the metal ions (Table 1).

Overall structure of the Mn_4CaO_5-cluster

Various lines of evidence have suggested the existence of mono- and di-μ-oxo-bridges linking the metal ions in the Mn_4Ca-cluster of OEC. However, the exact number and positions of the oxygen atoms were not known. In the 3.5 Å structure, 4 oxygen atoms were tentatively assigned in the Mn_4Ca-cluster [7], largely based on the requirement to link the metal ions, as the oxygen atoms are difficult to be distinguished from the electron density map at this resolution. Thus, in the 2.9 Å structure, no oxygen atoms were placed in the metal cluster [9]. In the 1.9 Å resolution structure, 5 oxygen atoms were identified to bridge the 5 metal ions for the first time, based on their omit map [21]. This yields a Mn_4CaO_5-cluster, as shown in Fig. 2A.

The overall shape of the Mn_4CaO_5-cluster revealed from the 1.9 Å structure resembles the shape of a distorted chair, with a distorted seat base formed by 3 Mn, 1 Ca,

and 4 oxygen atoms, and the back of the chair formed by the isolated 4th Mn and 1 oxygen atom. The distortion in the chair form is caused by the differences in the bond distances between Mn-O and Ca-O: While most of the Mn-O distances are within the range of 1.9-2.1 Å, the distances between 3 Mn atoms (Mn1, Mn3, Mn4) and one oxygen atom (O5) are in the range of 2.4-2.6 Å, which is significantly longer than the other, normal Mn-O distances. On the other hand, the Ca-O bond distances are in the range of 2.3-2.5 Å, which are longer than the normal Mn-O distances but comparable to that of Mn-O5 distances. The seat base of the structure thus showed a shape of distorted cubane-type, which has been suggested previously but the exact positions of each atoms could be determined only in the high resolution structure.

In addition to the 5 oxygen atoms, 4 water molecules were found to be associated with the Mn_4CaO_5-cluster [21]. Two of them are associated with Mn4 (W1, W2), whereas the other 2 are associated with the Ca atom (W3, W4) (Fig. 2A). The distances between the 2 water molecules and Mn4 are 2.1-2.2 Å, whereas those between water and Ca are 2.4-2.5 Å. No other water molecules were found to be associated with the other 3 Mn atoms, suggesting that at least one of the 4 water molecules serves as the substrates for water-oxidation. In relation to this, it is worth to mention that at least one of the substrate waters is bound already in the S_1-state [28, 29].

Among the 4 water molecules bound to the Mn_4CaO_5-cluster, W4 is directly hydrogen-bonded to Y_Z, the D1-Y161 residue mediating electron transfer between the PSII RC and the Mn_4CaO_5-cluster (Fig. 2B) [21]. W1-W3 are hydrogen-bonded to Y_Z indirectly through other 3 water molecules W5-W7. Notably, the distance between W7 and Y_Z is 2.6 Å, suggesting that it is a strong (low-barrier) hydrogen-bond. Y_Z is further hydrogen-bonded to D1-H190 with a short distance of 2.5 Å. The hydrogen-bond network further extends to D1-N298, and to the lumenal bulk phase through a number of water molecules and several hydrophilic or charged residues (not shown, see [21]). This strongly suggests the presence of a proton-coupled electron transfer (PCET) through Y_Z, in agreement with a number of previous reports suggesting the possible existence of this pathway [30-34].

The overall shape of the Mn_4CaO_5-cluster, the differences in the bond distances between different pairs of Mn-O, and between the pairs of Mn-O and Ca-O, and the water molecules found as ligands for the cluster, may have important consequences for

the mechanism of water oxidation and O-O bond formation. First of all, the presence of the Ca atom in the distorted cubane makes the OEC cubane-structure unique since so far only a symmetric 4 Mn cubane structure as well as a two-cubane structure formed by two 4-Mn cubanes, has been reported [35-37]. These structures have a shape of regular cubane, and are considered inactive or having low activity in catalyzing water-oxidation. The inclusion of Ca in the OEC resulted in a distorted cubane structure, which may constitute one of the reasons for the catalytic activity of OEC. Another significant feature of the Mn_4CaO_5-cluster structure is the remarkably longer bond distances between O5 and metal ions compared to those between other oxygen atoms and metal ions. This suggests a weak bonding of O5 within the cluster, implying a higher reactivity of this oxygen atom. Interestingly, 2 water molecules, W2 and W3, bound to Mn4 and Ca respectively, are within hydrogen-bond distances of O5 (Fig 2A). These results strongly suggest that 2 of the 3 species, W2, W3 and O5, provide the substrates for O-O bond formation during the water oxidation reaction.

Ligands for the Mn_4CaO_5-cluster

Previous studies have assigned most of the ligands for the Mn_4CaO_5-cluster [7-10]. Due to the limitations in resolution as well as the possible radiation damages, however, ambiguities existed regarding the exact ligand structure of the metal cluster, and the bond distances between the metal ions and their ligands were not determined accurately. Significant differences were also found in the ligation pattern between the 3.5 Å [7] and the 3.0 Å and 2.9 Å [8, 9] structures. While most of the carboxylate ligands served as mono-dentate ligands in the former structure, most of them were assigned as bi-dentate ligands in the latter structure. In the 1.9 Å structure, it is possible to assign all of the amino acid ligands to the Mn_4CaO_5-cluster unambiguously [21]. As shown in Fig. 3A, in total there are 6 carboxylate ligands and 1 His ligand; they are D1-D170, D1-E189, D1-E333, D1-D342, D1-A344, CP43-E354, and D1-H332. Among them, D1-D170, D1-E333, D1-D342, D1-A344, and CP43-E354 served as bi-dentate ligands, whereas D1-E189 and D1-His332 served as mono-dentate ligands. These amino acid ligands, combined with the oxo-bridges and water ligands, give rise to a saturating ligand environment for the metal cluster. As shown in Table 2, it became clear that there are 6 ligands for each of the 4 Mn atoms, and 7 ligands for the Ca atom [21].

Comparing with the ligation pattern reported in the 2.9 Å structure, two significant differences were found. One is regarding D1-E189, which was reported to serve as a possible bi-dentate ligand to Mn1 and Ca in the 2.9 Å structure, whereas it is assigned as a mono-dentate ligand to Mn1 in the 1.9 Å structure. One of the oxygen atoms of its carboxylate group has a distance of 3.3 Å to the Ca atom and thus is impossible to ligate to the Ca atom in the 1.9 Å structure. Another difference is regarding D1-D170, which was reported as a mono-dentate ligand to Mn4 with a distance of 2.4 Å, and the other oxygen of its carboxylate group has a distance of 2.9 Å to the Ca atom and therefore is considered to be not possible to ligate to the Ca atom in the 2.9 Å structure. In the 1.9 Å structure, while the bond distance of one oxygen of the D1-D170 carboxylate group to Mn4 is decreased to 2.1 Å, the other oxygen of the carboxylate group has a distance of 2.4 Å and therefore becomes to be ligated to the Ca atom. In addition to these major differences, the bond distances of each ligand to the metal ions were slightly different between the 2.9 Å and 1.9 Å structures, which were summarized in Table 3.

The structure and possible roles of 3 residues in the second coordination sphere of the metal cluster

In addition to the direct ligands to the Mn_4CaO_5-cluster described above, 3 residues were found to be located in the second coordination sphere of the cluster and may have direct interactions with the metal cluster. These 3 residues are D1-D61, D1-H337, and CP43-R357 (Fig. 4). Among these 3 residues, the imidazole ε-nitrogen of D1-H337 is hydrogen-bonded to O3 directly. One of the guanidinium η-nitrogen of CP43-R357 is hydrogen-bonded to both O2 and O4. These two residues may thus provide partial positive charges to compensate for some of the negative charges brought about by the oxo-bridges and carboxylate ligands of the metal cluster, thereby stabilizing the structure of the cluster. In other words, in the absence of these residues, some of the oxo-bridges may be unstable and collapsed due to attraction by the strong positive charges provided by the 5 metal ions. In addition, the other guanidinium η-nitrogen of CP43-R357 is hydrogen-bonded to both D1-D170 and D1-A344. One of the carboxylate oxygen of D1-D61 is directly hydrogen-bonded to W1, one of the water molecule bound to Mn4, and the other carboxylate oxygen of D1-D61 is hydrogen-bonded to W2 indirectly through two other water molecules W8 and W9 (Fig. 4). These

hydrogen-bonds may also be important for the stabilization of the metal cluster. These results are consistent with a variety of reports showing the importance of the above 3 residues in maintaining the oxygen-evolving activity based on mutagenesis and functional studies [38-42].

Binding sites of Cl^- ions

Previous studies have identified two Cl^--binding sites in the vicinity of the Mn_4CaO_5-cluster from the structural studies of Br^- and I^--substituted PSII [11,43]. Only one of these 2 sites, however, was visible in native PSII in the 2.9 Å structure [9], and it has been questioned whether both sites represented the native binding sites of Cl^- ions in PSII [44], as they are located 6-7 Å away from the Mn_4CaO_5-cluster. More importantly, while the Cl-1 binding site is surrounded by a positively charged residue D1-K317, no such residues have been found in the vicinity of the Cl-2 binding site, which was surrounded by hydrophilic residues with rather long distances [11,43]. This suggested that even if the Cl-2 binding site is indeed a site for Cl-binding, the binding of the anion in this site must be weak in native PSII, leading to the inability of observation of this site in the native structure at 2.9 Å resolution. In addition, there were some postulations that Cl^- may provide a direct ligand to the Mn_4CaO_5-cluster, as removal of Cl^- ions showed a remarkable effect on the activity of oxygen evolution as well as the properties of the metal cluster [45,46].

In the newly solved 1.9 Å structure, the two Cl-binding sites were clearly visible in the electron density map [21], which are located in the similar positions as those reported previously [11,43]. They were also confirmed by the anomalous difference-Fourier map taken at a wavelength of 1.75 Å, where Cl^- ions have a larger contribution than the "light atoms" constituting the amino acids. The anomalous difference-Fourier map also showed that there were no other Cl^- ions in the first coordination sphere of the Mn_4CaO_5-cluster, thereby excludes the possibility for Cl^- being a direct ligand to the metal ions in the OEC. This is in agreement with the above results that all of the 5 metal ions in the OEC have their valences saturated with ligands provided by oxo-bridges, amino acid residues, and water molecules, and do not need any additional ligands.

From the high resolution structure, the Cl-1 binding site is located 6.7 Å from Mn4,

and Cl-2 is located 7.4 Å away from Mn2 (Fig. 5). Both Cl^- ions are surrounded by 4 groups respectively. The only charged residue found among these groups is D2-K317, which has a distance of 3.3 Å to Cl-1 (Fig. 5). All other groups are either water or hydrophilic groups, and their distances to the two Cl-binding sites are rather long, suggesting that the 2 Cl^- ions are predominately bound by hydrogen-bonds. This structural feature suggests that binding of the two Cl^- ions in PSII is rather weak, in agreement with a variety of experimental results showing that Cl^- ions in PSII can be easily released by various treatments, resulting in the inactivation of oxygen evolution, and a simple addition of Cl^- ions into the medium results in the re-binding of Cl^- to PSII and the recovery of oxygen evolution (for reviews, see [45,46]).

In addition to D2-K317, the groups surrounding Cl-1 are the backbone nitrogen of D1-E333 and two water molecules. The 4 groups surrounding Cl-2 are backbone nitrogens of D1-N338 and CP43-E354, and 2 water molecules (Fig. 5). Thus, both Cl^--binding sites have a similar coordinating environment; namely, among the 4 groups surrounding each of the 2 Cl^--binding sites, 2 are water molecules and 2 are provided by amino acid residues. In particular, both D1-E333 and CP43-E354 have their side chain carboxylates coordinated to the Mn_4CaO_5-cluster as bi-dentate ligands, and their backbone nitrogen are associated with the two Cl^- ions. The two Cl^- ions may therefore function to maintain the structure of these two residues required for their stable binding to the Mn_4CaO_5-cluster. Release of these Cl^- ions may affect the stable coordination of these two residues to the Mn_4CaO_5-cluster, thereby resulting in an inactivation of oxygen evolution. Alternatively, the two Cl^- ions are located in the entrance of two possible proton exit paths where extensive hydrogen-bond networks existed starting from the Mn_4CaO_5-cluster to the lumenal bulk phase [7,9,21,47-50]. These suggest that the two Cl^- ions may also function in maintaining the proton exit pathways.

Additional Ca^{2+} and Cl^- binding sites

In addition to the 1 Ca atom present within the Mn_4CaO_5-cluster and 2 Cl^- ions found in the vicinity of the cluster, there are 3 additional Ca^{2+} and 1 additional Cl^- ions found in the high resolution structure (Fig. 6). These additional Ca^{2+} and Cl^- ions were confirmed by the anomalous difference-Fourier map taken at a wavelength of 1.75 Å. In addition, 1 additional Ca^{2+} was found in monomer B but not in monomer A, so we will

discuss the 3 Ca^{2+}-binding sites commonly found in both monomers in the following.

The 3 additional Ca^{2+} ions are all located in the lumenal side of PSII. One of them, Ca-1, is located in the surface of the β-barrel structure of PsbO toward the lumenal side, and has a distance of around 45 Å to the Mn_4CaO_5-cluster (Fig. 7A). This Ca^{2+} is coordinated by 7 groups; they are PsbO-N200, PsbO-Val201, PsbO-T138, and 4 water molecules. The location of this Ca^{2+} is different from the one reported previously [9,51], which was located in the region of PsbO toward the lumenal membrane surface and therefore is more close to the Mn_4CaO_5-cluster. In the high resolution density map, this Ca^{2+} was not found; instead, there is a water molecule in its vicinity which had a rather weak electron density without corresponding anomalous difference-Fourier signals (not shown).

The second Ca^{2+} is close to the lumenal surface and has a distance of around 40 Å to the Mn_4CaO_5-cluster. It has 7 ligands provided by PsbF-R45, a glycerol molecule serving as a bi-dentate ligand, and 4 water molecules. The presence of the glycerol molecule may be due to the inclusion of glycerol in the cryo-protectant solution, leading to the incorporation of this molecule into the crystal structure. Since glycerol is a hydrophilic molecule, we can assume that in native PSII, the position of glycerol is occupied by water molecules. Thus, Ca-2 may be associated with PSII rather weakly, as 6 out of its 7 ligands are occupied by water molecules in native PSII. A further weaker binding is found for Ca-3, which has only 4 ligands, among which, only 1 is provided by an amino acid (CP47-N438) and the other 3 are provided by water molecules. It has a distance of around 36 Å to the Mn_4CaO_5-cluster.

All of the above 3 Ca^{2+}-binding sites are located rather in the surface or periphery of the individual protein subunits, raising the question on whether these Ca^{2+}-binding sites represent the physiologically functional sites. Since Ca^{2+} is present in the crystallization solution [21,52], it is possible that they are incorporated into the complex during crystallization. A clear answer as to whether these Ca^{2+}-binding sites are physiologically functional may be obtained by examining the functional importance of the amino acid residues surrounding these Ca^{2+}-binding sites.

Different from the Ca^{2+}-binding sites, only 1 Cl^--binding site (Cl-3) was found in addition to the 2 Cl^--binding sites located in the vicinity of the Mn_4CaO_5-cluster, based on the anomalous difference Fourier-map taken at the 1.75 Å wavelength. Cl-3 was

located in the vicinity of PsbV and PsbU, and was surrounded by 6 water molecules in a position close to PsbU-K104, the C-terminal residue of PsbU (Fig. 8A). The fact that Cl-3 is supported only by water molecules suggests that its binding to this site is rather weak. It has a distance of around 25 Å to the Mn_4CaO_5-cluster. Interestingly, Cl-3 is located in the exit of a hydrogen-bond network from the Mn_4CaO_5-cluster to the lumenal surface (Fig. 8B), suggesting that this pathway may serve as one of anion supply pathways, or substrate-water inlet / proton exit pathways. The existence of this channel as possible water-inlet or proton-exit pathways has been suggested previously [49, 50].

The location of Cl-3 between PsbU and PsbV, in particular in the close vicinity to the C-terminus of the PsbU subunit, may suggest a physiological role of this site in oxygen evolution, since the relationship between Cl^- ions and extrinsic proteins has been well reported [53,54]. The growth rate of both *psb*U or *psbV* mutant from *Synechocystis* sp. PCC 6803 has been shown to be lower than that of the wild type strain in the absence of Ca^{2+} or Cl^-, suggesting a role of both PsbU and PsbV in maintaining the optimum ion (Ca^{2+} and Cl^-) environment required for oxygen evolution [55-57].

In conclusion, the high resolution structure of oxygen-evolving photosystem II analyzed at 1.9 Å resolution revealed for the first time the exact structure of the Mn_4CaO_5-cluster in which 5 oxygen atoms were found to serve as oxo-bridges linking the 5 metal ions. The overall shape of the metal cluster resembles a distorted chair, with a cubane-like chair base formed by 3 Mn, 1 Ca, and 4 oxygen atoms, and a chair back formed by a terminal Mn and an oxygen atom. Four water molecules were associated with the Mn_4CaO_5-cluster, 2 of them were associated with the terminal Mn atom and the other 2 were associated with the Ca atom. Thus, part of these 4 water molecules may serve as the substrate for water oxidation. All of these 4 water molecules were hydrogen-bonded either directly or indirectly to Y_Z, which connected to a hydrogen-bond network toward the lumenal bulk phase, suggesting a role of proton-coupled electron transfer in delivering the protons out of the reaction site. All of the ligands for the 5 metal ions were identified, some of which were found to have different ligation patterns than those reported previously. These structural features provide the basis for elucidation of the mechanisms of the water-oxidation and O-O

bond formation reaction catalyzed by PSII, one of the most important chemical reactions taking place on the earth.

Acknowledgements

This work was supported by a Grant-in-Aid for Creative Scientific Research, a GCOE program on Pico-biology at the University of Hyogo, and Grant-in-Aid for Scientific Research, from the Ministry of Education, Culture, Sports, Science and Technology of Japan, and a research grant from the Yamada Science foundation.

References

[1] T.J. Wydrzynski, K. Satoh, (eds), Photosystem II: The light-driven water:plastoquinone oxidoreductase, Springer (2005), Dordrecht, The Netherlands.

[2] J.-R. Shen, T. Henmi, N. Kamiya, Structure and Function of Photosystem II, In: P. Fromme (ed.) Structure of Photosynthetic Proteins, pp. 83-106 (2008), WILEY-VCH Verlag GmbH & Co KGaA, Weinheim.

[3] B. Kok, B. Forbush, M. McGloin, Cooperation of charges in photosynthetic oxygen evolution. I. A linear four step mechanism, Photochem. Photobiol. 11 (1970) 457-475.

[4] P. Joliot, Period-four oscillations of the flash-induced oxygen formation in photosynthesis, Photosynth. Res. 76 (2003) 65-72.

[5] G. Renger, T. Renger, Photosystem II: The machinery of photosynthetic water splitting, Photosynth. Res. 98 (2008) 53–80.

[6] A. Zouni, H.T. Witt, J. Kern, P. Fromme, N. Krauß, W. Saenger, P. Orth, Crystal structure of photosystem II from *Synechococcus elongatus* at 3.8 Å resolution, Nature 409 (2001) 739-743.

[7] K.N. Ferreira, T.M. Iverson, K. Maghlaoui, J. Barber, S. Iwata, Architecture of the photosynthetic oxygen-evolving center, Science 303 (2004) 1831-1838.

[8] B. Loll, J. Kern, W. Saenger, A. Zouni, J. Biesiadka, Towards complete cofactor arrangement in the 3.0 Å resolution structure of photosystem II, Nature 438 (2005) 1040-1044.

[9] A. Guskov, J. Kern, A. Gabdulkhakov, M. Broser, A. Zouni, W. Saenger, Cyanobacterial photosystem II at 2.9 Å resolution and role of quinones, lipids, channels and chloride, Nat. Struct. Mol. Biol. 16 (2009) 334-342 (2009).

[10] N. Kamiya, J.-R. Shen, Crystal structure of oxygen-evolving photosystem II from *Thermosynechococcus vulcanus* at 3.7-Å resolution, Proc. Natl. Acad. Sci. USA 100 (2003) 98-103.

[11] K. Kawakami, Y. Umena, N. Kamiya, J.-R. Shen, Location of chloride and its possible functions in oxygen-evolving Photosystem II revealed by X-ray crystallography, Proc. Natl. Acad. Sci. U.S.A. 106 (2009) 8567–8572.

[12] K. Kawakami, M. Iwai, M. Ikeuchi, N. Kamiya, J.-R. Shen, Location of PsbY in oxygen-evolving photosystem II revealed by mutagenesis and X-ray crystallography, FEBS Lett. 581 (2007) 4983-4987.

[13] J. Yano, J. Kern, K.-D. Irrgang, M.J. Latimer, U. Bergmann, P. Glatzel, Y. Pushkar, J. Biesiadka, B. Loll, K. Sauer, J. Messinger, A. Zouni, V.K. Yachandra, X-ray damage to the Mn_4Ca complex in single crystals of photosystem II: A case study for metalloprotein crystallography, Proc. Natl. Acad. Sci. USA 102 (2005) 12047-12052.

[14] M. Grabolle, M. Haumann, C. Müller, P. Liebisch, H. Dau, Rapid loss of structural motifs in the manganese complex of oxygenic photosynthesis by X-ray irradiation at 10-300 K, J. Biol. Chem. 281 (2006) 4580-4588.

[15] J. Yano, J. Kern, K. Sauer, M.J. Latimer, Y. Pushkar, J. Biesiadka, B. Loll, W. Saenger, J. Messinger, A. Zouni, Y. K. Yachandra, Where water is oxidized to dioxygen: structure of the photosynthetic Mn_4Ca cluster, Science 314 (2006) 821-825.

[16] P.E.M. Siegbahn, A structure-consistent mechanism for dioxygen formation in photosystem II, Chem. Eur. J. 14 (2008) 8290-8302.

[17] P.E.M. Siegbahn, An energetic comparison of different models for the oxygen evolving complex of photosystem II, J. Am. Chem. Soc. 131 (2009) 18238-18239.

[18] P.E.M. Siegbahn, Structures and energetics for O_2 formation in photosystem II, Acc. Chem. Res. 42 (2009) 1871-1880.

[19] E.M. Sproviero, J.A. Gascón, J.P. McEvoy, G.W. Brudvig, V.S. Batista, Quantum mechanics/molecular mechanics study of the catalytic cycle of water splitting in

photosystem II, J. Am. Chem. Soc. 130 (2008) 3428-3442.

[20] E.M. Sproviero, J.P. McEvoy, J.A. Gascón, G.W. Brudvig, V.S. Batista, Computational insights into the O_2-evolving complex of photosystem II, Photosynth. Res. 97 (2008) 91-114.

[21] Y. Umena, K. Kawakami, J.-R. Shen, N. Kamiya, Crystal structure of oxygen-evolving photosystem II at 1.9 A resolution, Nature, in press (2011).

[22] S. Zein, L.V. Kulik, J. Yano, J. Kern, Y. Pushkar, A. Zouni, V.K. Yachandra, W. Lubitz, F. Neese, J. Messinger, Focusing the view on nature's water-splitting catalyst, *Phil. Trans. R. Soc.* B 363 (2008) 1167–1177.

[23] H. Dau, A. Grundmeier, P. Loja, M. Haumann, On the structure of the manganese complex of photosystem II: extended-range EXAFS data and specific atomic-resolution models for four S-states, Phil. Trans. R. Soc. B 363 (2008) 1237-1244.

[24] H. Dau, M. Haumann, The manganese complex of photosystem II in its reaction cycle—basic framework and possible realization at the atomic level. Coord. Chem. Rev. 252 (2008) 273–295.

[25] Y. Pushkar, J. Yano, P. Glatzel, J. Messinger, A. Lewis, K. Sauer, U. Bergmann,, V. K. Yachandra, Structure and orientation of the Mn_4Ca cluster in plant photosystem II membranes studied by polarized range-extended X-ray absorption spectroscopy, J. Biol. Chem. 282 (2007) 7198–7208.

[26] R.M. Cinco, K.L.M. Holman, J.H. Robblee, J. Yano, S.A. Pizarro, E. Bellacchio, K. Sauer, V. K. Yachandra, Calcium EXAFS establishes the Mn–Ca cluster in the oxygen-evolving complex of photosystem II, Biochemistry 41 (2002) 12928–12933.

[27] R. M. Cinco, J.H. Robblee, J. Messinger, C. Fernandez, K.L.M. Holman, K. Sauer, V.K. Yachandra, Orientation of calcium in the Mn_4Ca cluster of the oxygen-evolving complex determined using polarized strontium EXAFS of photosystem II membranes, Biochemistry 43 (2004) 13271–13282.

[28] W. Hillier, T. Wydrzynski, The affinities for the two substrate water binding sites in the O_2 evolving complex of photosystem II vary independently during S-state turnover, Biochemistry 39 (2000) 4399-4405.

[29] G. Hendry, T. Wydrzynski, The two substrate-water molecules are already bound

to the oxygen-evolving complex in the S_2 state of photosystem II, Biochemistry 41 (2002) 13328-13334.

[30] C.W. Hoganson, G.T. Babcock, A metalloradical mechanism for the generation of oxygen from water in photosynthesis, Science 277 (1997) 1953-1956.

[31] C. Tommos, G.T. Babcock, Proton and hydrogen currents in photosynthetic water oxidation, Biochim. Biophys. Acta 1458 (2000) 199-219.

[32] J.S. Vrettos, J. Limburg, G.W. Brudvig, Mechanism of photosynthetic water oxidation: combining biophysical studies of photosystem II with inorganic model chemistry, Biochim. Biophys. Acta 1503 (2001) 229-245.

[33] G. Renger, Photosynthetic water oxidation to molecular oxygen: apparatus and mechanism, Biochim. Biophys. Acta 1503 (2001) 210-228.

[34] A.-M.A. Hays, I.R. Vassiliev, J.H. Golbeck, R.J. Debus, Role of D1-His190 in the proton-coupled oxidation of tyrosine Y_Z in manganese-depleted Photosystem II. Biochemistry 38 (1999) 11851-11865.

[35] M.D. Godbole, M. Kloskowski, R. Hage, A. Rompel, A. M. Mills, A. L. Spek, E. Bouwman, Highly efficient disproportionation of dihydrogen peroxide: Synthesis, structure, and catalase activity of manganese complexes of the salicylimidate ligand, Eur. J. Inorg. Chem. 2005 (2005) 305-313.

[36] M.D. Godbole, O. Roubeau, A.M. Mills, H. Kooijman, A.L. Spek, E. Bouwman High-nuclearity manganese and iron complexes with the anionic ligand methyl salicylimidate, Inorg. Chem. 45 (2006) 6713-6722.

[37] D.M. Robinson, Y.B. Go, M. Greenblatt, G.G. Dismukes, Water oxidation by lambda-MnO2: catalysis by the cubical Mn4O4 subcluster obtained by delithiation of spinel LiMn2O4, J. Am. Chem. Soc. 132 (2010) 11467-11469.

[38] P.J. Nixon, B. Diner, Analysis of water-oxidation mutants constructed in the cyanobacterium *Synechocystis* sp. PCC 6803, Biochem. Soc. Trans. 22 (1994) 338-343.

[39] H.-A. Chu, A.P. Nguyn, R.J. Debus, Amino acid residues that influence the binding of manganese or calcium to Photosystem II. 1. The lumenal inter-helical domains of the D1 polypeptide, Biochemistry 34 (1995) 5839-5858.

[40] H.J. Hwang, P. Dilbeck, R.J. Debus, R.L. Burnap, Mutation of arginine 357 of the CP43 protein of photosystem II severely impairs the catalytic S-state cycle of the

H_2O oxidation complex, Biochemistry 46 (2007) 11987-11997.

[41] R.J. Debus, Protein ligation of the photosynthetic oxygen-evolving center, Coord. Chem. Rev. 252 (2008) 244–258.

[42] R.J. Service, W. Hillier, R.J. Debus, Evidence from FTIR difference spectroscopy of an extensive network of hydrogen bonds near the oxygen-evolving Mn_4Ca cluster of Photosystem II involving D1-Glu65, D2-Glu312, and D1-Glu329, Biochemistry 49 (2010) 6655–6669.

[43] J.W. Murray, K. Maghlaoui, J. Kargul, N. Ishida, T.-L. Lai, A. W. Rutherford, M. Sugiura, A. Boussac, J. Barber, X-ray crystallography identifies two chloride binding sites in the oxygen evolving centre of Photosystem II, Energy Environ. Sci. 1 (2008) 161–166.

[44] A. Guskov, A. Gabdulkhakov, M. Broser, C. Glöckner, J. Hellmich, J. Kern, J. Frank, F. Müh, W. Saenger, A. Zouni. Recent progress in the crystallographic studies of photosystem II, ChemPhysChem. 11(2010) 1160-1171.

[45] K. Olesen, K. L.E. Andreasson, The function of the chloride ion in photosynthetic oxygen evolution, Biochemistry 42 (2003) 2025–2035.

[46] H. Popelková, C.F. Yocum, Current status of the role of Cl^- ion in the oxygen-evolving complex, Photosynth. Res. 93 (2007) 111-121.

[47] J.W. Murray, J. Barber, Structural characteristics of channels and pathways in photosystem II including the identification of an oxygen channel, J. Struct. Biol. 159 (2007) 228–237.

[48] F.M. Ho, S. Styring, Access channels and methanol binding site to the $CaMn_4$ cluster in Photosystem II based on solvent accessibility simulations, with implications for substrate water access, Biochim. Biophys. Acta 1777 (2008) 140–153.

[49] A. Gabdulkhakov, A. Guskov, M. Broser, J. Kern, F. Müh, W. Saenger, A. Zouni, Probing the accessibility of the Mn_4Ca cluster in photosystem II: Channels calculation, noble gas derivatization, and cocrystallization with DMSO, Structcure 17 (2009) 1223–1234.

[50] S. Vassiliev, P. Comte, A. Mahboob, D. Bruce, Tracking the flow of water through photosystem II using molecular dynamics and streamline tracing, Biochemistry 49 (2010) 1873–1881.

[51] W.J. Murray, J. Barber, Identification of a calcium-binding site in the PsbO protein of photosystem II, Biochemistry 45 (2006) 4128-4130.

[52] J.-R. Shen, N. Kamiya, Crystallization and the crystal properties of the oxygen-evolving photosystem II from *Synechococcus vulcanus*, Biochemistry 39 (2000) 14739-14744.

[53] I. Enami, A. Okumura, R. Nagao, T. Suzuki, M. Iwai M, J.-R. Shen, Structures and functions of the extrinsic proteins of photosystem II from different species, Photosynth. Res. 98 (2008) 349-363.

[54] J.L. Roose, K.M. Wegener, H.B. Pakrasi, The extrinsic proteins of Photosystem II, Photosynth. Res. 92 (2007) 369-387.

[55] J.-R. Shen, M. Ikeuchi, Y. Inoue, Analysis of the psbU gene encoding the 12-kDa extrinsic protein of photosystem II and studies on its role by deletion mutagenesis in *Synechocystis* sp. PCC 6803, J. Biol. Chem. 272 (1997) 17821-17826.

[56] J.-R. Shen, M. Qian, Y. Inoue, R.L. Burnap, Functional characterization of *Synechocystis* sp. PCC 6803 Δ*psb*U and Δ*psb*V mutants reveals important roles of cytochrome *c*-550 in cyanobacterial PSII, Biochemistry 37 (1998) 1551-1558.

[57] N. Inoue-Kashino, Y. Kashino, K. Satoh, I. Terashima, H.B. Pakrasi, PsbU provides a stable architecture for the oxygen-evolving system in cyanobacterial photosystem II, Biochemistry 44 (2005) 12214-12228.

Table 1. Comparison of the Mn-Mn and Mn-Ca distances between the present and previous structures (Å). The distances from the 3 structures were taken from the average values of the two monomers within a dimer.

Structures (pdb, ref)	1.9 Å (3ARC, 15)	Berlin (3BZ1, 3BZ2, 8)	London (1S5L, 6)
Mn1-Mn2	2.8	2.7	2.7
Mn2-Mn3	2.9	2.8	2.7
Mn3-Mn4	3.0	3.2	3.3
Mn1-Mn3	3.3	3.2	2.7
Mn1-Mn4	5.0	5.3	5.1
Mn2-Mn4	5.4	5.8	3.3
Mn1-Ca	3.5	3.4	3.3
Mn2-Ca	3.4	3.2	3.4
Mn3-Ca	3.4	3.3	3.4
Mn4-Ca	3.8	4.6	3.9

Table 2. Ligands of the Mn_4CaO_5-cluster determined at 1.9 Å resolution.

Mn1	Mn2	Mn3	Mn4	Ca
D1-Glu189	D1-Asp342	D1-Glu333	D1-Asp170	D1-Asp170
D1-His332	D1-Ala344	CP43-Glu354	D1-Glu333	D1-Ala344
D1-Asp342	CP43-Glu354	O2	O4	O1
O1	O1	O3	O5	O2
O3	O2	O4	W1	O5
O5	O3	O5	W2	W3
				W4

Table 3. Comparison of the ligand distances of the Mn_4CaO_5-cluster between the 1.9 Å and 2.9 Å structures. The distances from the 1.9 Å structure are the average of two PSII monomers in the dimer. The variations between the two monomers were in the range of 0.1 Å. Values in italics represent the breakage of the bonds.

	Distances (Å)			Distances (Å)	
	1.9 Å	2.9 Å		1.9 Å	2.9 Å
Mn1-D1/E189-OE2	1.9	1.8	Mn3-D1/E333-OE1	2.1	2.2
Mn1-D1/H332-NE2	2.2	2.3	Mn3-CP43/E354-OE2	2.2	2.3
Mn1-D1/D342-OD2	2.3	2.7	Mn4-D1/D170-OD2	2.1	2.5
Mn2-D1/D342-OD1	2.2	2.3	Mn4-D1/E333-OE2	2.2	2.7
Mn2-D1/A344-OXT	2.0	1.7	Ca-D1/D170-OD1	2.4	*2.9*
Mn2-CP43/E354-OE1	2.2	2.6	Ca-D1/A344-O	2.6	2.5
			Ca-D1/E189-OE2	*3.3*	2.5

Figure legends

Fig. 1. Positions of the metal ions in the Mn4CaO5-cluster determined at 1.9 Å resolution. A. Electron density for each of the metal ions obtained from the 2Fo-Fc map contoured at 8.0 σ. B. Distances (Å) between each pair of Mn-Mn and Mn-Ca determined from the 1.9 Å structure. C. Comparison of the positions of the metal ions between the 1.9 Å, 2.9 Å (Berlin), and 3.5 Å (London) structures. The Mn atoms from the Berlin structure were shown as crosses in purple, and the Ca atom was shown as a cross in yellow, whereas the Mn atoms from the London structure was shown as cyan crosses and the Ca atom as green atom.

Fig. 2. Structure of the Mn_4CaO_5-cluster determined at 1.9 Å resolution. A. Structure of the metal cluster with oxo-bridges and water ligands. The bond distances were shown in Å. Hydrogen bonds were depicted as dashed lines. B. Hydrogen-bond network linking the Mn_4CaO_5-cluster and Y_Z, and further from Y_Z to the opposite side.

Fig. 3. Ligand structure of the Mn_4CaO_5-cluster. A. Ligand structure of the metal cluster determined at 1.9 Å resolution. Residues from D1 were colored in green, and that from CP43 was colored in cyan. B. Comparison of the ligand structure between the 1.9 Å and 2.9 Å structure. The 4 Mn atoms from the 2.9 Å structure were depicted as purple crosses, and the Ca atom as yellow cross. The color of the amino acids from the 1.9 Å structure were the same as in A, whereas those of D1 from the 2.9 Å structure were depicted in blue, and that of CP43 in dark salmon. Bond distances for D1-D170 and D1-E189 to the metal ions from the 2.9 Å structure were shown.

Fig. 4. Structure of three residues located in the second coordination sphere of the Mn_4CaO_5-cluster. The three residues D1-D61, D1-H337, and CP43-R357 are depicted in bold sticks. Hydrogen-bond distances are depicted in Å.

Fig. 5. Structure of the two Cl^--binding sites in the vicinity of the Mn_4CaO_5-cluster. Hydrogen-bond distances are depicted in Å.

Fig. 6. Additional Ca^{2+} and Cl^- binding sites found in the 1.9 Å resolution structure. The PSII monomer was shown as a cartoon model from which, the pigment and other cofactors were omitted.

Fig. 7. Detailed structure of the 3 additional Ca^{2+}-binding sites. A. Ca-1 binding site coordinated by PsbO and water molecules. B. Ca-2 binding site coordinated by PsbF and a glycerol (GOL) molecule, and 4 water molecules. The color codes for the protein subunits are as follows: pink, PsbF; yellow orange, PsbV; and green, PsbC. C. Ca-3 binding site coordinated by PsbB and 3 water molecules. PsbB was shown as orange, and PsbO was shown as light blue.

Fig. 8. Detailed structure of the Cl-3 binding site. A. Coordination environment of the Cl-3. Color codes for the protein subunits are as follows: pink, PsbU; dark yellow, PsvV; orange, CP47; and blue, D2. B. A hydrogen-bond network connecting the Mn_4CaO_5-cluster and Cl-3.

Fig. 1

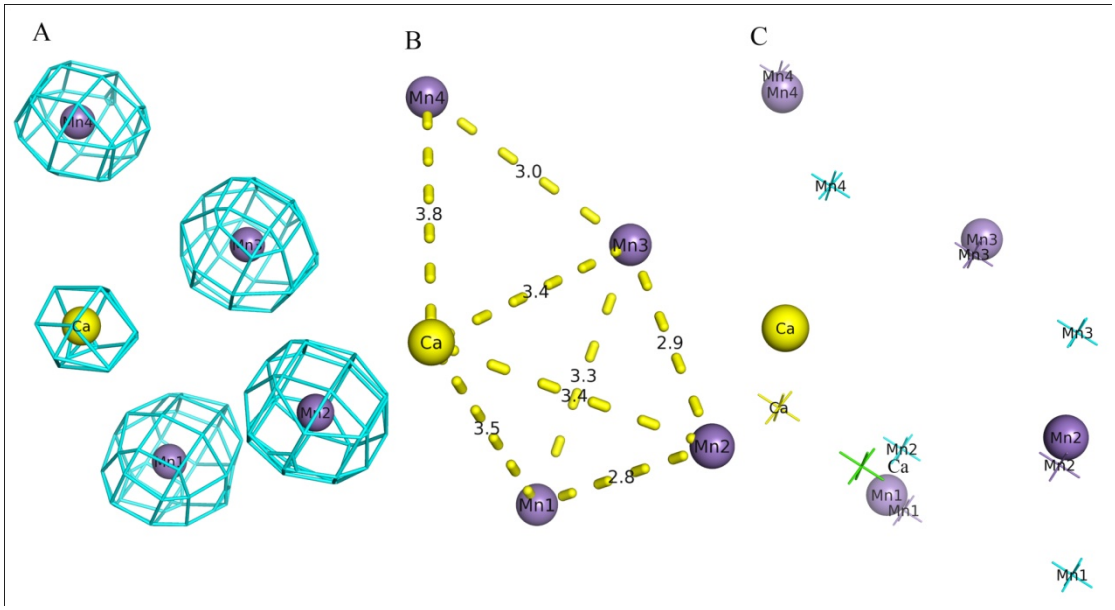

Fig. 2

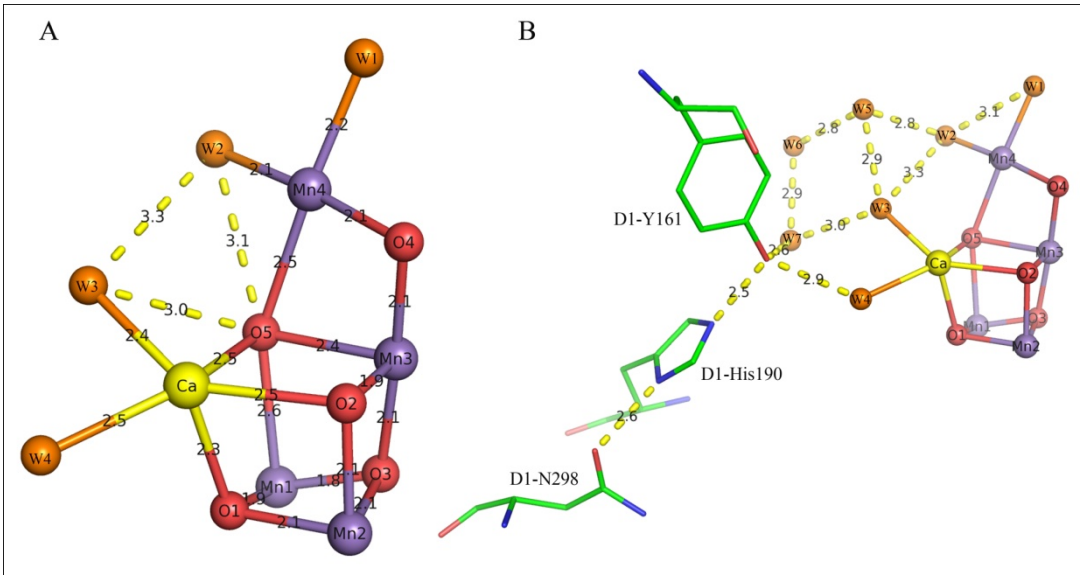
A
B
W1
W2
Mn4
O4
W3
O5
Mn3
Ca
O2
W4
Mn1
O3
O1
Mn2
D1-Y161
D1-His190
D1-N298

Fig. 3

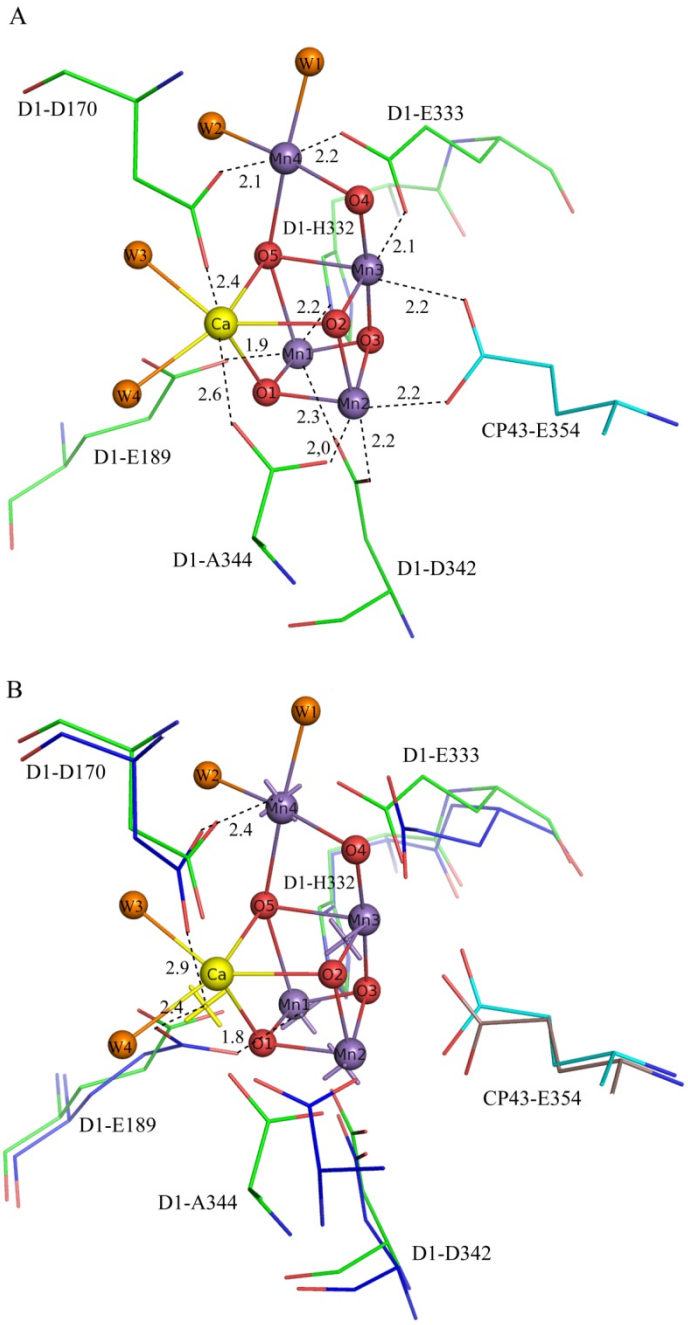
A
W1
D1-D170
D1-E333
W2
Mn4
2.2
2.1
O4
D1-H332
2.1
W3
O5
Mn3
2.4
2.2
2.2
Ca
O2
2.2
O3
1.9
Mn1
W4
2.6
O1
Mn2
2.2
2.3
CP43-E354
2,0
2.2
D1-E189
D1-A344
D1-D342
B
W1
D1-E333
D1-D170
W2
Mn4
2.4
O4
D1-H332
W3
O5
Mn3
2.9
Ca
O2
O3
2.4
Mn1
1.8
W4
O1
Mn2
CP43-E354
D1-E189
D1-A344
D1-D342

Fig. 4

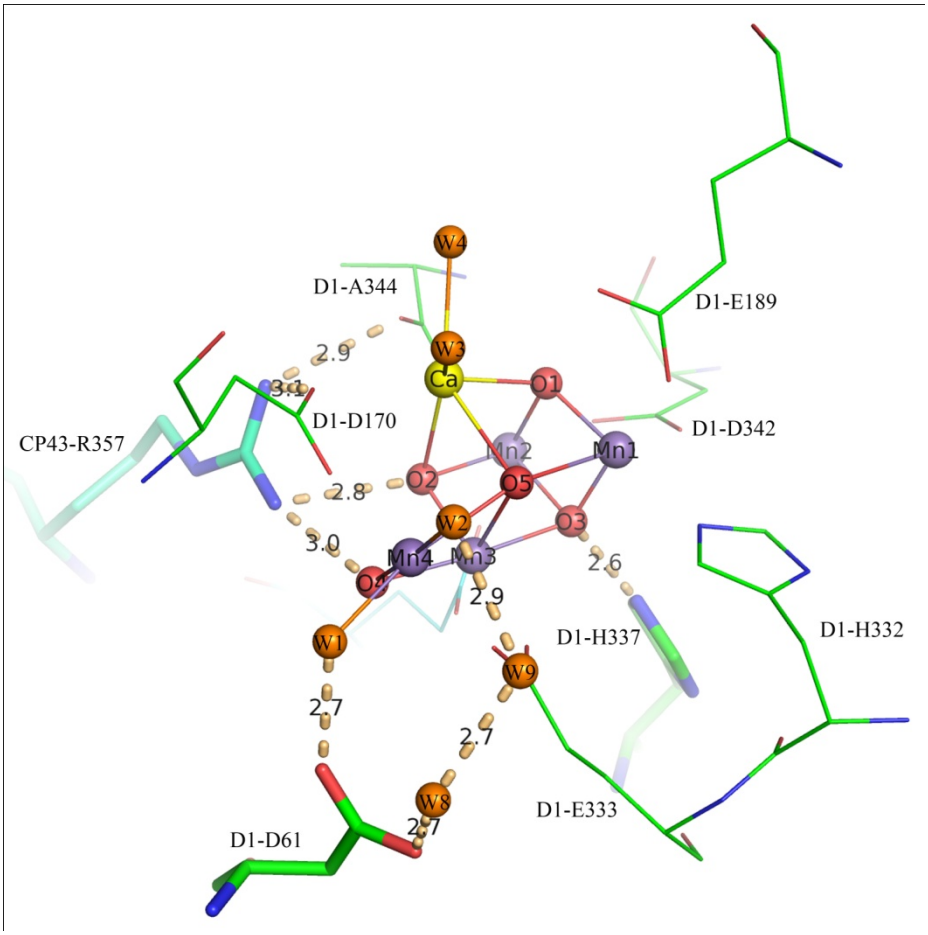
W4
D1-A344
D1-E189
W3
2.9
Ca
O1
3.1
D1-D170
D1-D342
CP43-R357
Mn2
Mn1
O2
O5
2.8
W2
O3
3.0
Mn4
Mn3
2.6
O4
2.9
D1-H337
D1-H332
W1
W9
2.7
2.7
W8
D1-E333
2.7
D1-D61

Fig. 5

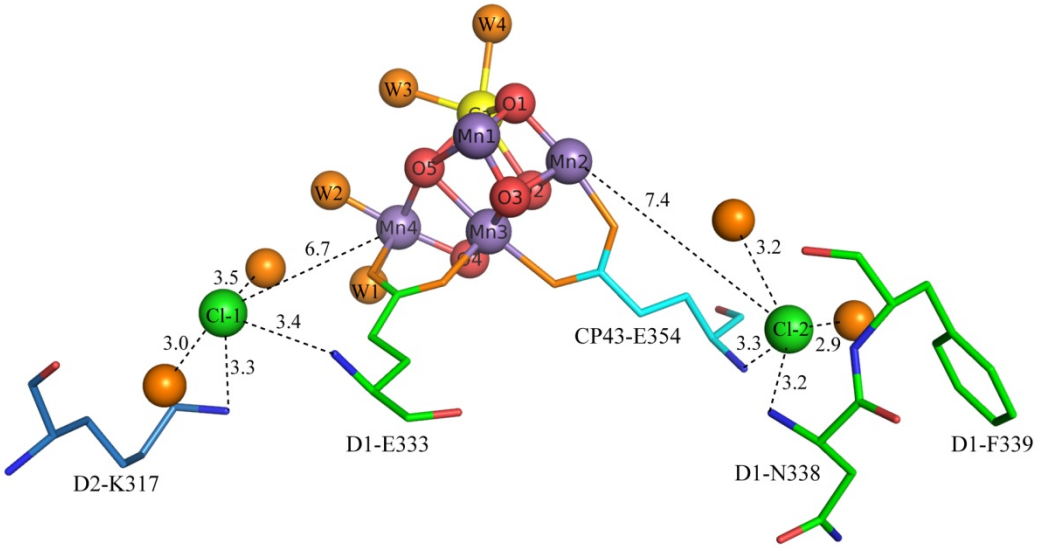
W4
W3
O1
Mn1
O5
Mn2
W2
O3
Mn4
Mn3
W1
7.4
3.2
6.7
3.5
Cl-1
3.4
3.0
3.3
CP43-E354
3.3
Cl-2
2.9
3.2
D1-E333
D2-K317
D1-N338
D1-F339

Fig. 6

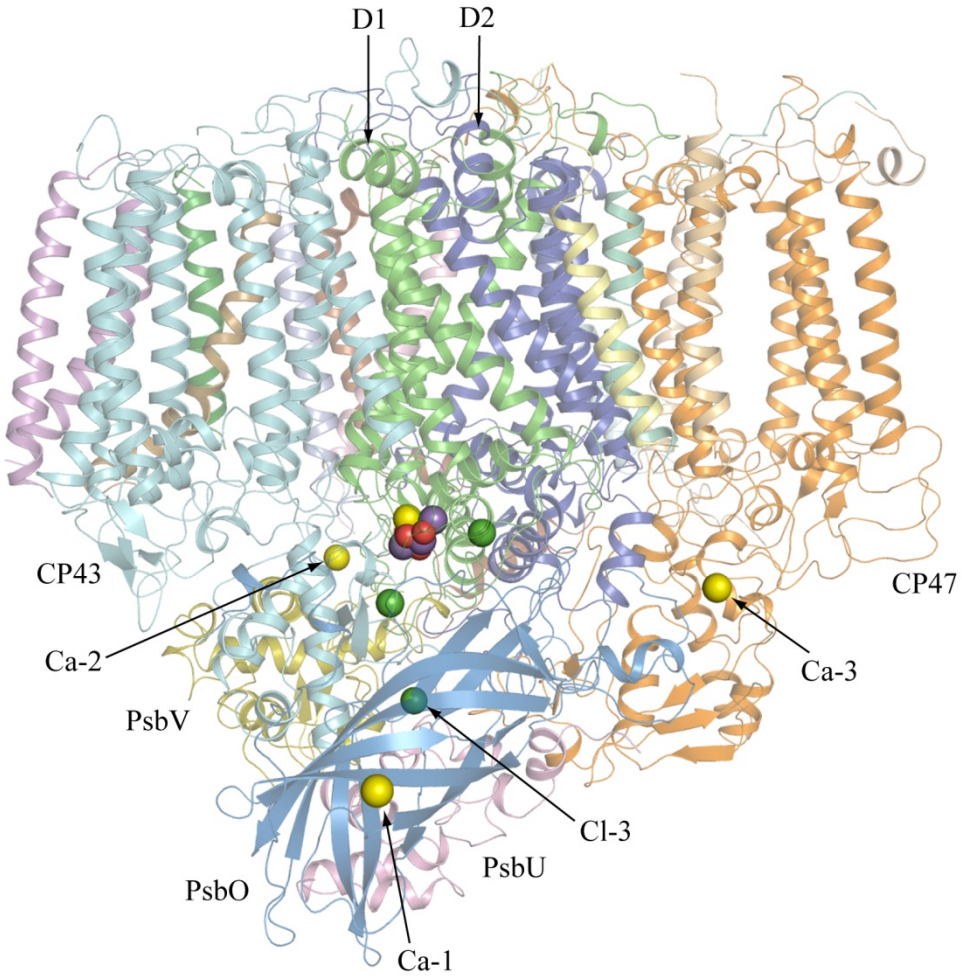

Fig. 7

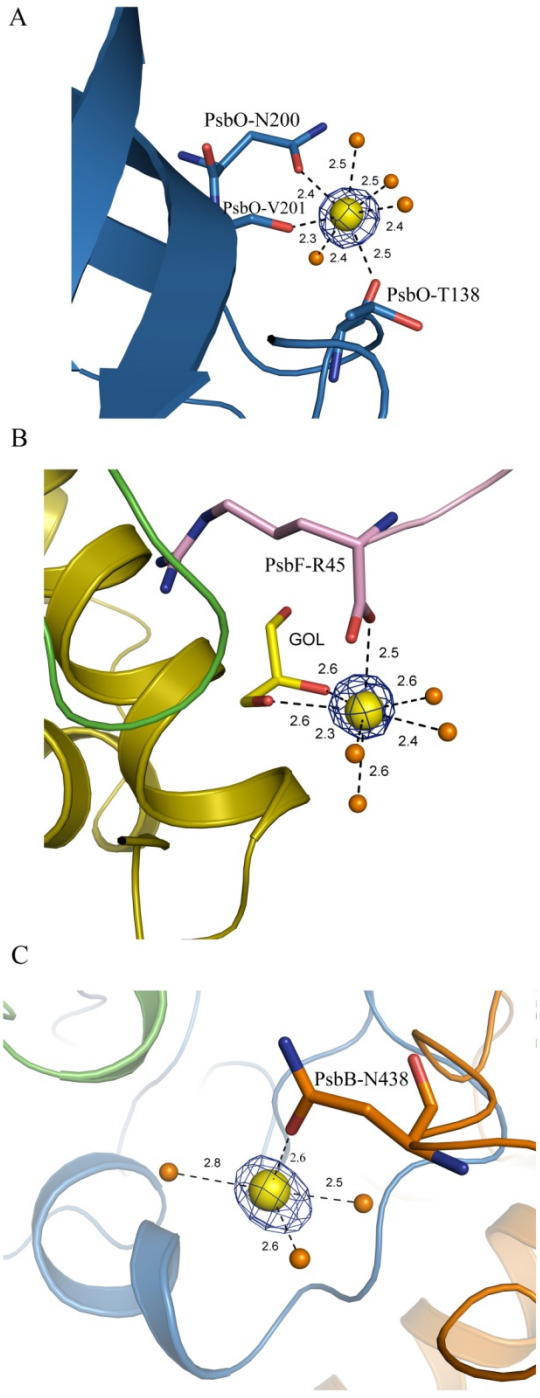
A
PsbO-N200
PsbO-V201
PsbO-T138
2.5
2.5
2.4
2.4
2.3
2.4
2.5
B
PsbF-R45
GOL
2.5
2.6
2.6
2.6
2.3
2.4
2.6
C
PsbB-N438
2.8
2.6
2.5
2.6

Fig. 8

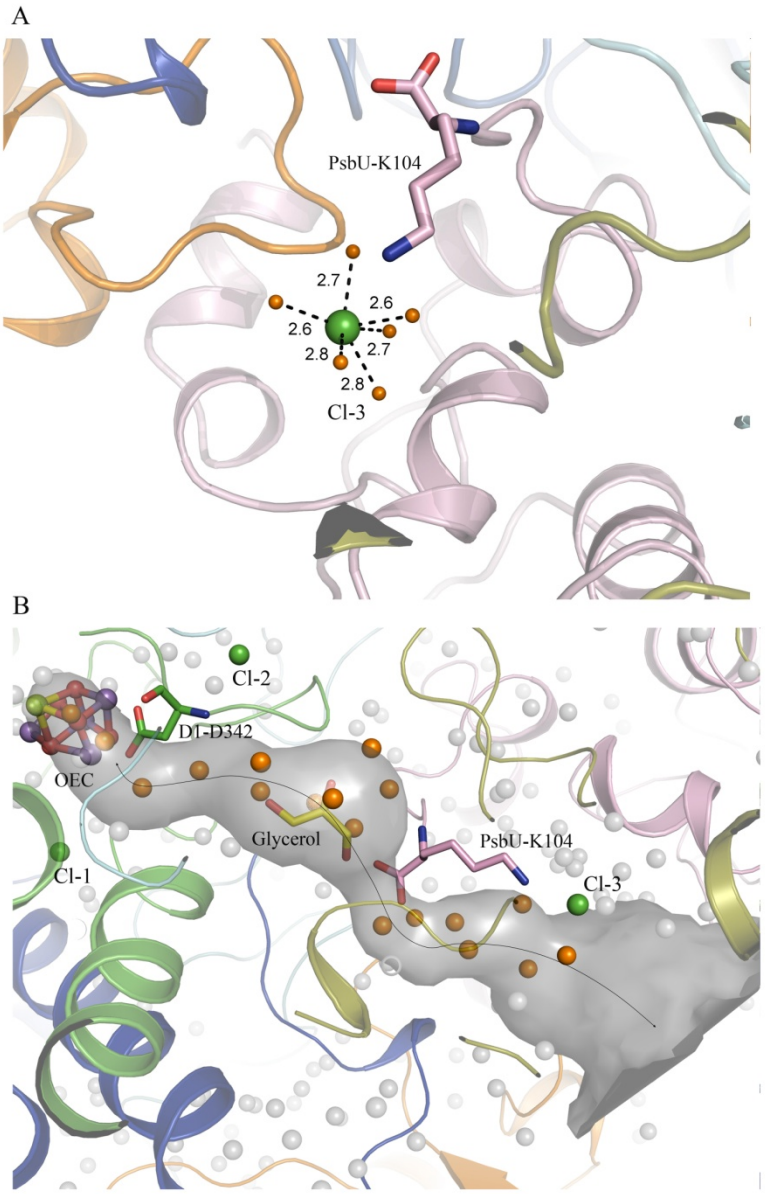
A
PsbU-K104
2.7
2.6
2.6
2.8
2.7
2.8
Cl-3
B
Cl-2
D1-D342
OEC
Glycerol
PsbU-K104
Cl-1
Cl-3